Publishing House
AKAPIT

COMPUTER METHODS IN MATERIALS SCIENCE

Informatyka w Technologii Materiałów

Vol. 10, 2010, No. 2

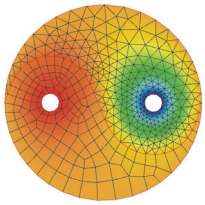

OPTIMIZATION OF DEEP DRAWING PROCESS FORMING PARAMETERS FOR MAGNESIUM ALLOYS

VICTOR B. WATITI*, GEORGE N. LABEAS

Laboratory of Technology and Strength of Materials, Faculty of Mechanical and Aeronautical Engineering, School of Engineering, University of Patras
Panepistimioupolis Rion, 265 00 Patras, Greece
**Corresponding Author: vwatiti@mech.upatras.gr*

Abstract

Formability of Magnesium alloys is limited especially at room temperature due to their hexagonal close packed (HCP) structure. At room temperature (RT), the critical resolved shear stress for non basal slip systems is much greater than those for basal slips. As only basal systems may contribute to plastic deformation, magnesium alloys have limited formability at RT. However, increased formability is observed at higher temperatures ranging between 150°C and 300°C due to the activation of additional slip planes. Additionally, it has been observed that the formability is very sensitive to strain rates. In this paper experimental methods and Finite Element (FE) analysis are applied for the development of a methodology based on strain energy density theory for determination of the forming limits of magnesium alloys AZ31 and WE43. Based on the developed methodology optimal forming parameters in a deep drawing forming process, namely punch radius, temperature, profile radius and forming depth, are determined.

Key words: Finite Elements, Forming Limits, Strain energy density, Magnesium alloys

1. INTRODUCTION

Recently, magnesium alloys have been widely applied in the automobile, electronics and partly in the aerospace industry due to their lightweight and high specific strength properties, e.g. Mordike and Ebert (2001) and Furuya et al. (2000). However forming of magnesium parts is not easy mainly due to their hexagonal close packed (HCP) structure. At RT, the critical resolved shear stress for non-basal slip systems is much higher compared to that for basal slips; as only basal systems may contribute to plastic deformation, magnesium alloys have limited formability at RT. However, increased formability is observed at higher temperatures ranging between 150°C and 200°C due to the activation of additional slip planes.

Although the principal manufacturing process for magnesium parts has been die casting, recently press forming processes are generally used due to their competitive productivity and performance. The most common press forming process applied is the deep drawing forming process. Deep drawing is a cold press forming process in which a flat blank of sheet metal is shaped by the action of a punch forcing the metal into a die cavity, as shown in figure 1. Deep drawing differs from other cold press forming processes in that the depth of the formed part can be greater than its diameter.

In the deep drawing process of sheet metals, the forming limit is determined by the onset of necking and predicted by analysis of tensile instability. However in the case of magnesium alloys, the application of these theories is limited, because fracture occurs

 ISSN 1641-8581

with limited or no necking at all. Therefore, new and more accurate theories should be applied for precise prediction of formability. Many efforts have been performed to study the deep drawing process of magnesium alloys. Takuda et al. (1999) used FE analysis to determine the formability of AZ31, but limited their analysis to RT conditions Chen et al. (2003), Zhang et al. (2007) and Ren et al. (2009) carried out experimental and FE analysis of the deep drawing of square cups of AZ31 at room and high temperatures, but no comparison has been made to any other alloy. Nguyen and Bapanapalli (2009) developed a methodology for the prediction of failure during forming for AZ31 at RT. Yang et al. (2008) investigated the formability of annealed magnesium AZ31 without mentioning anything on the forming parameters.

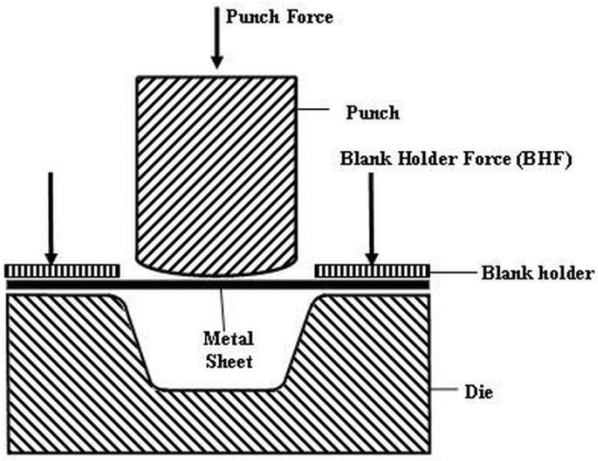

Fig. 1. *Representation of the deep drawing process.*

In the present paper experimental results and Finite Element (FE) simulations are used in the development of a methodology based on strain energy density theory for the prediction of forming limits of magnesium alloys at various forming temperatures and the determination of optimal forming conditions for the deep drawing process of magnesium alloys AZ31 and WE43.

2. FORMING LIMITS

In order to define the formability of sheet metallic materials, the Forming Limits are widely applied. A forming limit can be determined experimentally, analytically or numerically. Analytically, theories based on diffuse necking proposed by Swift (1952), localized necking introduced by Hill (1952) and thickness imperfection developed by Marciniak and Kuczynski (1971) can be used. These theories may be applied to forming of complicated geometries, where strains and stresses required are calculated using Finite Element Methods (FEM) and failure initiation using ductile fracture criteria.

2.1. Ductile fracture criteria

Ductile fracture criteria that are usually applied in sheet metal forming processes have been developed based on different approaches. The most common approaches state that the occurrence of ductile fracture is usually determined by the stress and strain conditions imposed during the forming process. The most widely used criteria are presented hereunder.

– Cockcroft and Latham (1968) and Brozzo et al. (1972), proposed a failure criterion of the form:

$$\int_0^{\varepsilon_f} \frac{2}{3}\left(1-\frac{\sigma_h}{\sigma_{\max}}\right)^{-1} d\varepsilon = C_1 \qquad (1)$$

– Norris et al. (1978) proposed a fracture criterion based on plastic strain:

$$\int_0^{\varepsilon_f} \frac{d\varepsilon}{1-c\sigma_h} = C_2 \qquad (2)$$

Where $c=\dfrac{1}{3.1\sigma_F}$

– Oh et al. (1979) modified the Cockroft and Latham (1968) criterion as follows:

$$\int_0^{\varepsilon_f} \frac{\sigma_{\max}}{\sigma_{eqv}} d\varepsilon = C_3 \qquad (3)$$

– Oyane et al. (1980) proposed a criterion based on the stress and strain histories during the forming process, which is of the form:

$$\int_0^{\varepsilon_f} \left(\frac{\sigma_h}{\sigma_{eqv}} + C_4\right) d\varepsilon = C_5 \qquad (4)$$

– Atkins (1981) modified the criterion proposed by Norris et al. (1978) in order to take into account the material behavior:

$$\int_0^{\varepsilon_f} \frac{1+(1/2L)}{1-c\sigma_h} d\varepsilon = C_6 \qquad (5)$$

Where $L=\dfrac{d\varepsilon_1}{d\varepsilon_2}$ and $c=\dfrac{1}{3.1\sigma_F}$

In eq. (1) – (5) ε is the strain at the critical point, ε_f is the equivalent strain at which fracture occurs, σ_h

is the hydrostatic stress, σ_{max} is the maximum normal stress, σ_{eqv} the equivalent stress, σ_F is the yield strength, while C_1 - C_6 are material constants.

In the present work a generic failure criterion based on the critical strain energy density value is applied. In Sih's work (1985) a failure criterion based on the accumulation of the strain energy density is proposed, which has mainly been applied for the prediction of crack propagation in fracture mechanics. A modification of this criterion, as appears in the following eq. (6), is proposed to be applied in metal forming processes:

$$\left(\frac{dW}{dV}\right)_{Critical} = C_7 = \int_0^{\varepsilon_f} \sigma^* d\varepsilon \qquad (6)$$

In eq. (6) ε_f is the equivalent strain at which fracture occurs, σ^* is the maximum equivalent tensile stress, W the virtual work, V the metal sheet unit volume, while C_7 is a material constant.

During the sheet metal deformation attention is paid on the fracture of the sheet element when the strain energy density reaches a critical value. Local instability of the elements with the critical strain energy leads to the onset of fracture.

At different strain rates or temperatures, the critical strain energy density is calculated by applying the trapezoidal rule on the corresponding stress-strain curve. The trapezoidal rule is of the form:

$$C = \varepsilon_f \left(\frac{R_P + R_m}{2}\right) \qquad (7)$$

In eq. (7) R_p is the yield strength and R_m the tensile strength of the alloy.

The fracture point on the metal sheet is then determined by combining the calculated stress and strain history from the FE model with the fracture criterion. Rewriting the Sih (1989) criterion, an integral of I_{Sih} is defined as:

$$I_{Sih} = \frac{1}{C_7} \int_0^{\varepsilon_f} \sigma^* d\varepsilon \qquad (8)$$

Using σ^* and $d\varepsilon$ obtained by the finite element simulation, the integral I_{Sih} is calculated for each element and deformation step. At any given stage of the deformation process, the stresses and strains are calculated and compared with the critical value C_7, which is considered to be a material property. The condition of fracture is satisfied when and where the integral I_{Sih} becomes equal to unity.

3. NUMERICAL SIMULATION OF THE DEEP DRAWING PROCESS

The commercial FE code ANSYS has been used for the process simulation. For the modeling of the metal blank, element type 'Solid 45' is used, which is suitable for three-dimensional (3-D) modeling of solid structures; it is defined by eight nodes having three degrees of freedom at each node, the translations in the nodal *x, y* and *z* directions. The element has plasticity, creep, swelling, stress stiffening, large deflection and large strain capabilities. It should be noted that 3-D solid elements are selected for the present simulation due to the need of an accurate calculation of the through-the-thickness strain, which is required for the determination of the ductile fracture criteria constants and is also important in the calculation of the blank thickness reduction.

The interface phenomena due to the contact between punch – metal sheet, blank holder – metal sheet and metal sheet – die are simulated using element type 'Conta175'. For the modeling of the punch, the die and the blank holder element type 'Targe170' is used.

The simulation refers to the experimental tests performed in the frame of the European project AEROMAG (2006), comprising: a flat punch with a diameter of 10 mm and a profile radius r_p = 1 mm, 0.5 mm thick metal blank with a diameter of 25 mm, a blank holder with external diameter 25 mm and internal diameter 16 mm and a die with internal and external diameter 14 and 25 mm respectively. The experimentally determined Critical Punch Depth and max. forming time at RT are 1.6 mm and 93s respectively. The developed FE model is schematically shown in figure 2.

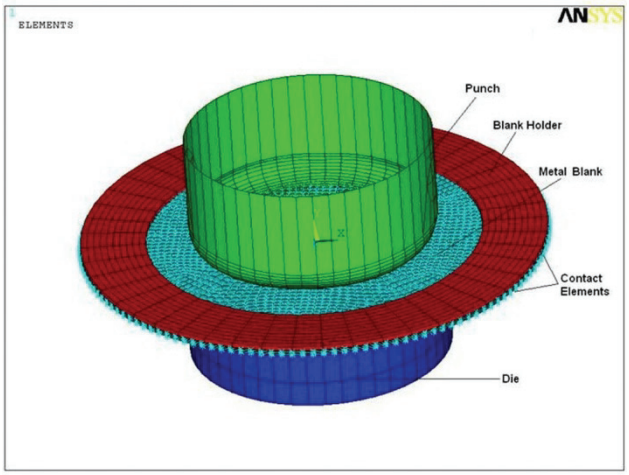

Fig. 2. *FE simulation model for the deep drawing process.*

The materials used in this study are Magnesium alloys AZ31 and WE43. For the coefficient of friction between the tools and the metal blank an average value of 0.2 was used, based on the parametric study with respect to temperature and contact conditions for AZ31 alloys by Ceretti et al. (2008), it has been shown that the coefficient of friction varies between 0.1-0.3 for the specific deep drawing case, while the Blank Holding Force (*BHF*) is calculated using Siebel equation, Gotoh et al. (2003). During the deep drawing process the *BHF* plays an important role, as its variation during the forming progression controls the deformation of the different areas of the blank and affects the fracture area. Siebel equation is of the form:

$$P = 0.025\left\{(\beta - 1)^3 + 0.005\delta\right\}S_t, \qquad BHF = PA \qquad (9)$$

In eq. (9), P is the blank holding pressure, β the drawing ratio (initial blank diameter/punch diameter), δ the relative punch diameter (punch diameter/initial thickness), S_t the tensile strength of the metal blank and A the effective area of the blank holder.

The FE model of the metal blank, which comprises 18018 nodes and 24091 elements, is shown in figure 3.

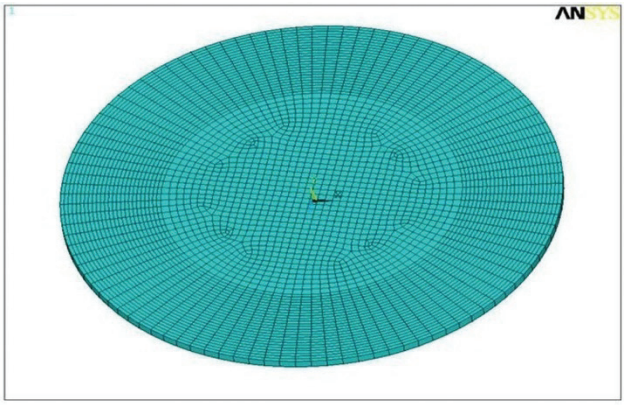

Fig. 3. *Finite element representation of the metal blank.*

It can be observed from figure 3 that the area where the blank is under compression due to application of the *BHF*, the FE mesh is denser in order to increase the accuracy of the calculated strain and stress results.

The simulation process is carried out at RT and elevated temperatures (100°C to 400°C). The mechanical properties of the two alloys (AZ31 and WE43) used are based on experiments carried out in the frame of AEROMAG (2006) and are presented in figure 4 and table 1.

Tensile tests to determine the mechanical properties of the magnesium alloys were carried out at the Institut National Polytechinique de Grenoble (INPG). In order to perform the tests, the sample was clipped and placed into a furnace until the temperature is stabilized to the desired one; consequently, tensile tests were carried out at the desired strain rate until the specimen failure. The yield stress is determined at the point at which the stress-strain curve deviates from linear ($\varepsilon = 0.2\%$). The strain rate sensitivity index is also determined.

Table 1. *Mechanical properties of AZ31 and WE43 in the L and LT direction at RT, AEROMAG (2006).*

	AZ31	**WE43**
Tensile strength (MPa)		
L	264	302
LT	263	256
Elongation (%)		
L	20.00	4.68
LT	19.45	12.17
K- value (MPa)	427	398
Work hardening coefficient, n		
L	0.162	0.11
LT	0.197	0.1
Normal Anisotropy, R		
L	5	2.5
LT	2.75	2.25
Strain rate sensitivity		
L	0.01	0.01

Like any other alloy, Magnesium alloys have a distinct grain structure alignment. The grain structure alignment is defined in three perpendicular directions: L – Longitudinal, LT – Transverse and ST Short transverse. In this case the L direction is the direction the magnesium sheet is rolled while the LT direction is in the plane perpendicular to the L direction.

For the simulation of the non linear material properties, the anisotropic hardening option in combination with the yield criterion proposed by Hill (1952) is used. The Anisotropic (ANISO) option allows for different multi linear stress-strain behavior in the material *x, y* and *z* directions as well as different behavior in tension, compression and shear. The Hill anisotropy option is combined with the ANISO option in order to simulate plasticity of the metal blank.

The Hill criterion (1952) is combined with the Swift (1952) hardening law in order to predict the yielding process and determine the effect of strain rate. The anisotropic yield criterion proposed by Hill and applied in this case is of the form:

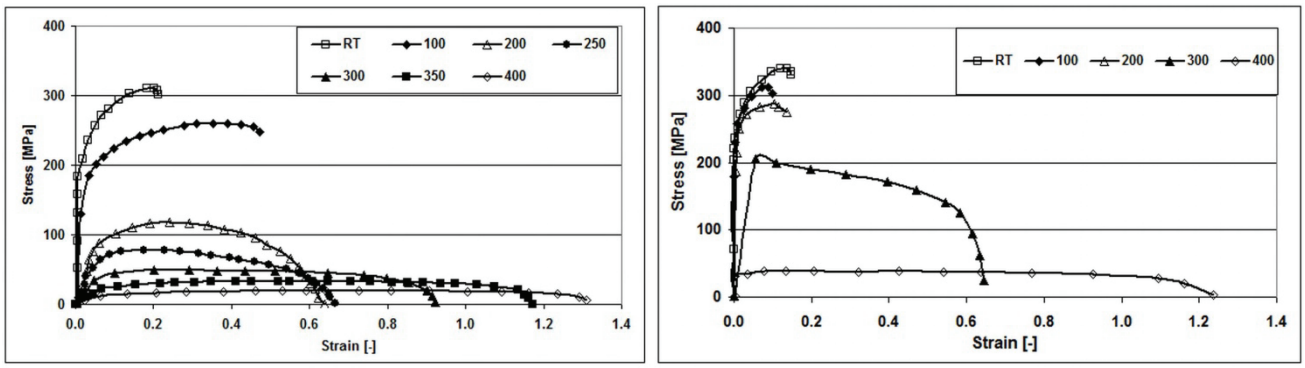

Fig. 4. *Mechanical properties at RT and high temperatures, (a) AZ31 and (b) WE 43, AEROMAG(2006).*

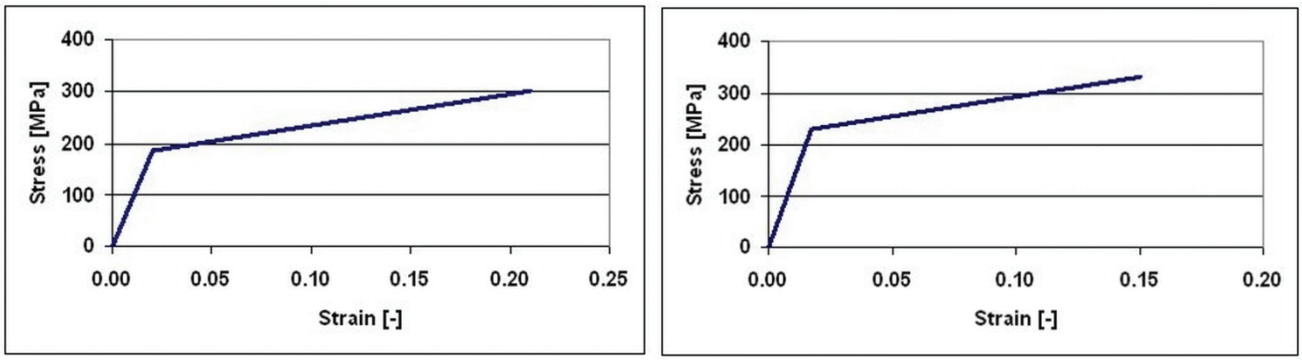

Fig. 5. *Non-linear stress – strain (σ – ε) curves idealized for the FE simulation, (a) AZ31 and (b) WE 43.*

$$2\sigma_{Eqv} = F(\sigma_y - \sigma_z)^2 + G(\sigma_z - \sigma_x)^2 + H(\sigma_x - \sigma_y)^2 + 2L\tau_{yz}^2 + 2M\tau_{zx}^2 + 2N_{xy}^2 \qquad (10)$$

In eq. (10) $\sigma_{eqv.}$ is the equivalent stress at yield, *F, G, H, L, M* and *N* are constants specific to the anisotropy state of the material and *x, y, z* are the principal anisotropic axes.

The constants in the Hill criterion are determined by:

$$F = \frac{1}{2}\left(\frac{1}{R_{22}^2} + \frac{1}{R_{33}^2} - \frac{1}{R_{11}^2}\right),$$
$$G = \frac{1}{2}\left(\frac{1}{R_{33}^2} + \frac{1}{R_{11}^2} - \frac{1}{R_{22}^2}\right),$$
$$H = \frac{1}{2}\left(\frac{1}{R_{11}^2} + \frac{1}{R_{22}^2} - \frac{1}{R_{33}^2}\right), \qquad (11)$$
$$L = \frac{3}{2R_{23}^2}, M = \frac{3}{2R_{31}^2}, \; N = \frac{3}{2R_{12}^2}$$

The yield stress ratios can be rewritten as function of the Lankford constants in the form:

$$R_{11} = R_{13} = R_{23} = 1, \quad R_{22} = \sqrt{\frac{r_{90}(r_0+1)}{r_0(r_{90}+1)}},$$
$$R_{33} = \sqrt{\frac{r_{90}(r_0+1)}{r_0 + r_{90}}}, \; R_{12} = \sqrt{\frac{3r_{90}(r_0+1)}{(2r_{90}+1)\cdot(r_0+r_{90})}} \qquad (12)$$

r_0 and r_{90} represent the anisotropy coefficient in the rolling (L) and lateral directions (LT) of the alloy respectively.

Swift equation is given by:

$$\sigma = K\varepsilon^n \dot{\varepsilon}_{eff}^m \qquad (13)$$

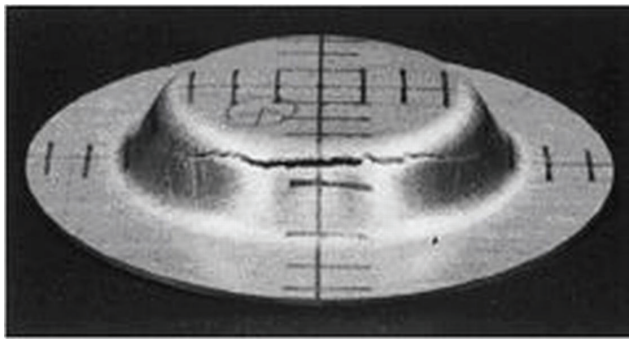

Fig. 6. *Fracture initiation observed in the test at around 7.9 mm; after Takuda et al (1999).*

In eq. (13) K is the strength coefficient, ε equivalent strain, n the hardening exponent, $\dot{\varepsilon}_{eff}$ equivalent strain rate and m the strain rate sensitivity index.

4. VERIFICATION OF THE MODEL

For the validation of the deep drawing simualtion model, numerical results are compared to experimental results at RT. The initial verification is carried out using the experimental work carried out by Takuda et al. (1999). The dimensions of the tool used are: flat punch with a diameter of 60 mm and a profile radius r_p = 4 mm, 0.6 mm thick metal blank with a diameter of 75 mm and a die with internal and external diameter 65 mm and 75 mm respectively. The experimentally achieved Critical Punch Depth (CPD) is 7.9 mm (at RT).

In figure 6, the experimentally derived deformed shape of the specimen after the deep drawing tests is presented, from which the fracture location can also be observed, at a CPD of 7.9 mm.

In the course of the simulation process, two integrals are calculated:

- I_{Oyane} – based on Takuda et al. (1999),
- I_{Sih} – Sih Criterion with C_7 = 45 MJ calculated from the trapezoidal rule.

In figure 7, the evolution of the above two fracture integrals, based on FE analysis are presented. The I_{Sih} integral is calculated based on the proposed strain energy density criterion, while the Oyane criterion is calculated based on the FE model verified by experimental results carried out by Takuda et al. (1999). The horizontal and vertical axes indicate the radial position from the metal blank center, while the values of the integrals are calculated at the corresponding radial positions, respectively.

From figure 7, it can be observed that the CPD calculated by the I_{Oyane} is 7.9 mm, while the I_{Sih} integral predicts the CPD to be 8.1 mm. The difference between the I_{Oyane} calculated by Takuda et al. (1999) based on a verified FE model and the I_{Sih} integral for the point of fracture is 2.5%. This shows that for the specific forming process the Sih (1980) strain energy density criterion predicts the fracture process with sufficient accuracy; therefore the I_{Sih} integral will be used hereafter for the optimization of the forming process.

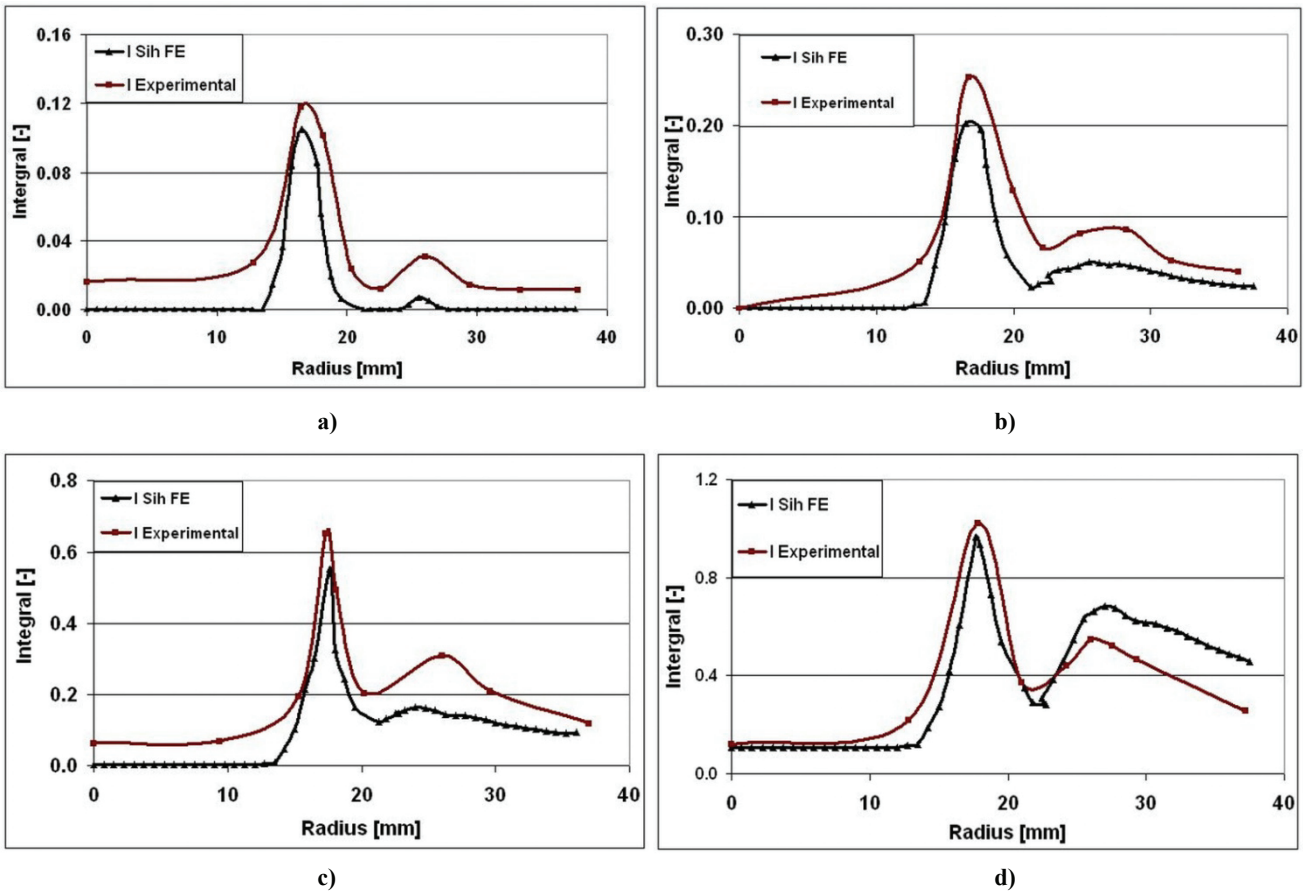

Fig. 7. *I_{Oyane} and $I_{Sih\ FE}$ integral at forming depth of 2 mm (a), 4 mm (b), 6 mm (c) and 7.9 mm (d).*

5. OPTIMIZATION OF THE DEEP DRAWING FORMING PROCESS

Having verified the simulation model, a FE analysis is carried out to investigate the effect of strain rate sensitivity and the most important deep drawing parameters, i.e., the forming temperature, punch radius and punch profile radius on the formability of AZ31 and WE43 alloys.

5.1. Temperature effect on formability

The maximum depth of deformation before fracture was used as an index of formability. The effect of forming temperature on the formability is then examined. In figure 8, the maximum depth of displacement of the metal blank before the prediction of fracture at different temperatures is presented.

From figure 8, it can be observed that at room temperature, the formability of the alloy is minimal, i.e. CPD is predicted at 2 mm, while as the temperature rises, the formability is improving up to a temperature of around 300°C, after which the formability drops again. The decrease of the formability at temperatures above a limit is attributed to the lower work hardening exponent at high temperatures that induces local thinning on the wall of the circular cup.

5.2. Strain Rate effect on formability

It should also be mentioned that the formability of Mg alloys is very sensitive to the strain rate. In table 2, the C_7 constant of the failure criterion (eq. 8) for different forming temperatures and at two strain

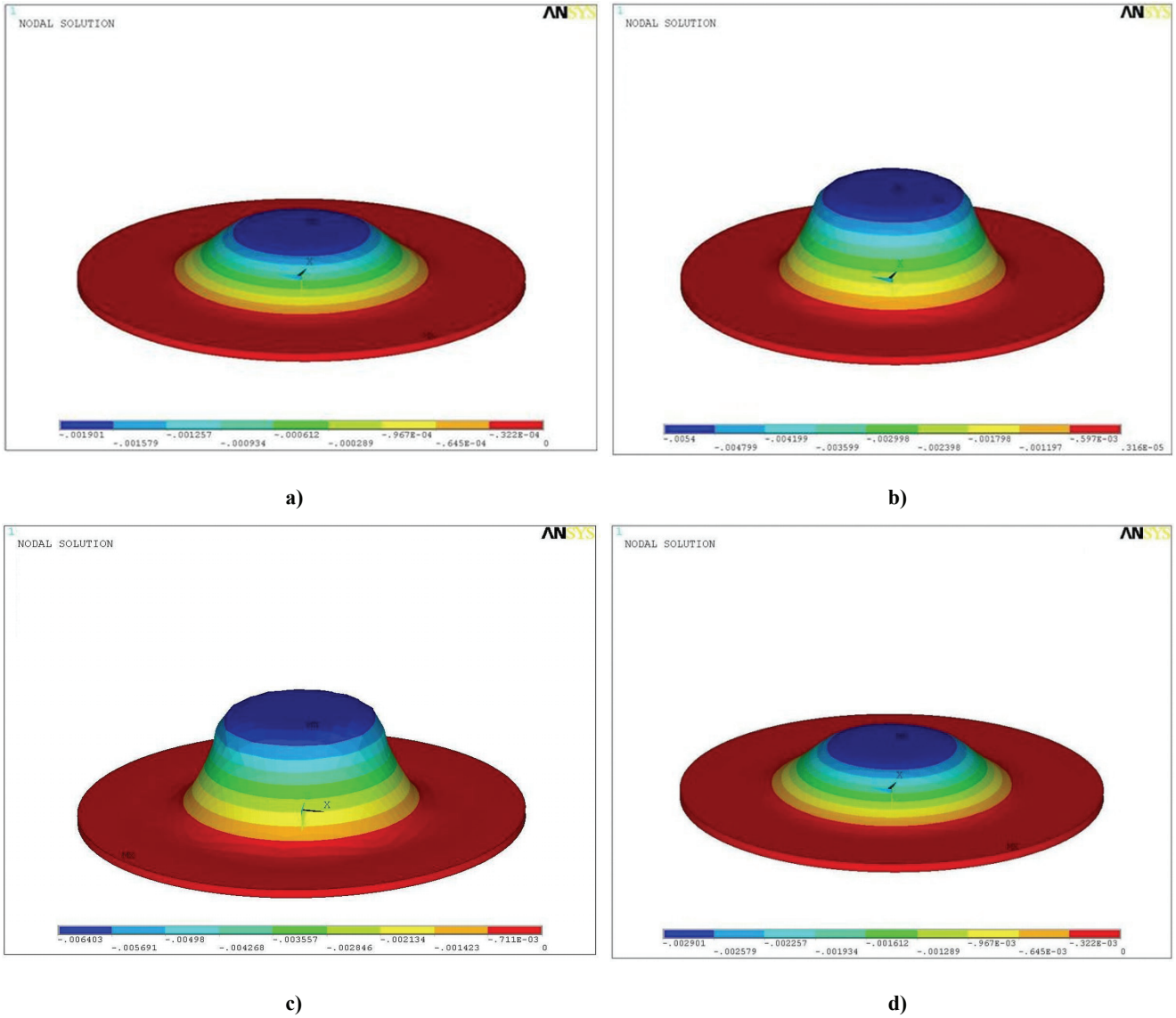

Fig. 8. *(a) Deformed FE shape of the deep drawing cup at CPD: (a) 1.9 mm at RT, (b) 5.4 mm at 200°C, (c) 6.4 mm at 300°C and (d) 2.9 mm at 400°C for AZ31 alloy.*

rates (strain rate 1 equal to $6 \cdot 10^{-4} s^{-1}$ and strain rate 2 equal to $5 \cdot 10^{-4} s^{-1}$) are presented.

Table 2. *Strain energy density values at different strain rates.*

Temperature [°C]	Strain rate 1		Strain rate 2	
	AZ31[MJ]	WE43[MJ]	AZ31[MJ]	WE43[MJ]
RT	45.2	26.7	44.9	26.1
100	70.8	43.4	57.2	42.7
200	98.2	64.2	72.5	52.3
300	101.8	51.3	98.0	45.2
400	22.9	19.2	21.2	18.8

Having determined the C_7 constants for the different temperatures and strain rates, the effect of the strain rate on formability is examined. In figure 9 the relationship between the forming temperature and the maximum drawing depth is shown.

It can be observed from figure 9, that formability is a function of the strain rate and forming temperature. At the high strain rate the optimum temperature for AZ31 is around 300°C for AZ31 and around 260°C for WE43. At a lower strain rate the optimum forming temperature drops to almost 200°C for AZ31 and 240°C for WE43.

5.2. Effect of punch radius (r_p) and profile radius on formability

The effect of the punch radius on the formability of the cup is studied. The punch radius is varied between 4 mm and 7 mm. In figure 10, a plot of the punch radius as a function of the CPD is presented.

From figure 10, it can be observed that a smaller punch radius reduces the formability. This can be attributed to the fact that a smaller punch radius restrains the material from being stretched equally in

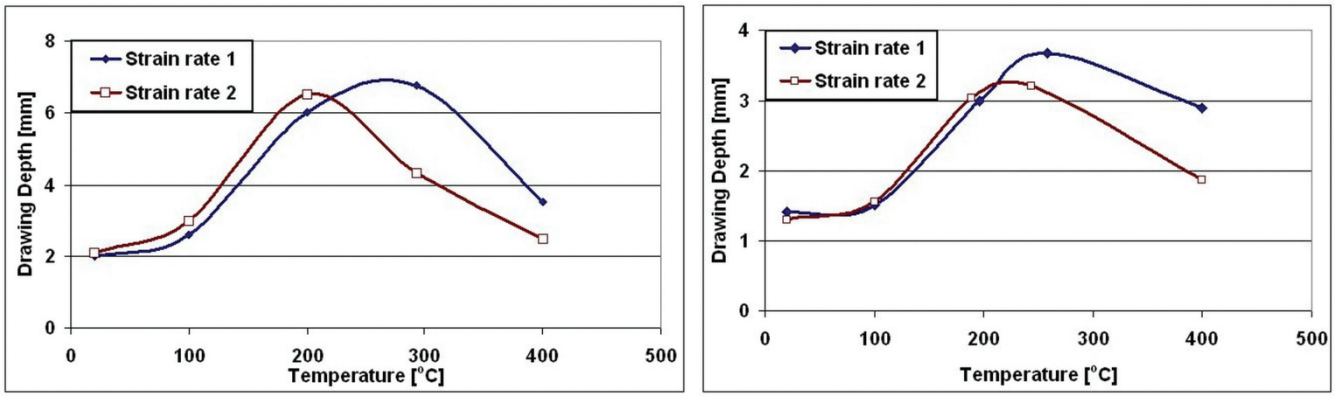

a) b)

Fig. 9. *Forming temperature versus Critical Punch Depth for two strain rate levels (a) for AZ31 and (b) for WE43.*

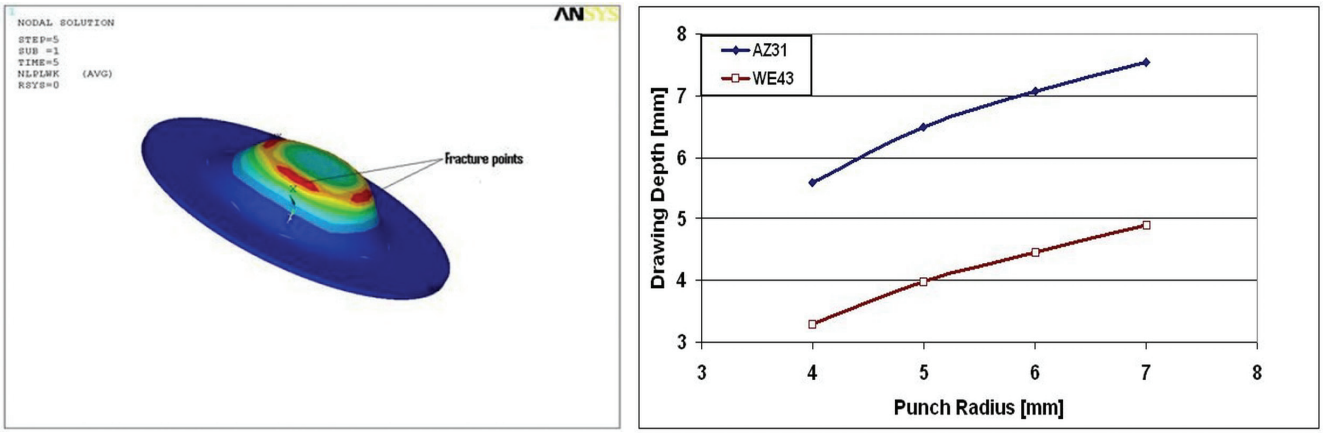

a) b)

Fig. 10. *(a) Deformed shape showing fracture points for punch radius 5 mm for AZ31 and (b) punch radius versus predicted drawing depth for AZ31 and WE43.*

both directions, which results in a dramatic increase in major strains causing early fracture.

The effect of the profile radius for AZ31 and WE43 are studied for values between 0.5 mm and 4 mm. The relationship between the punch profile radius and the forming depth is shown in figure 11.

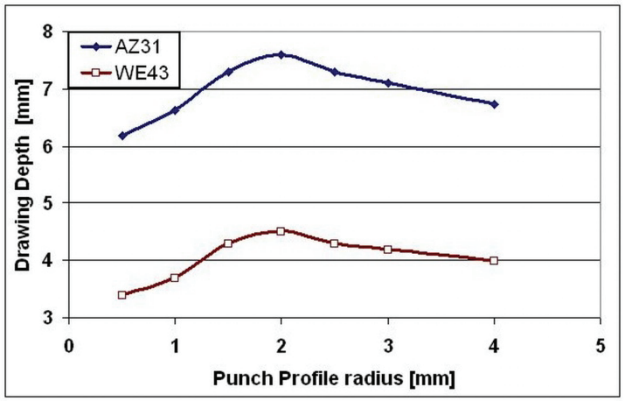

Fig. 11. *Relationship between die profile radius and drawing depth.*

From figure 11, it can be observed that there exists an optimum punch profile radius of 2 mm. When the punch profile radius is above 2 mm the draw depth reduces.

6. CONCLUSIONS

The formability of magnesium alloys AZ31 and WE 43 is studied in the present paper using numerical simulation of the forming process supported by experimental results. In order to predict the initiation of fracture, a fracture mechanics criterion proposed by Sih (1980) is appropriately modified for application fracture criterion in the case of forming. The rational of the criterion used is that the initiation of fracture is determined when the accumulated strain energy density in the metal reaches a critical value, which is calculated from the basic material mechanical properties. It is clear from both the experimental and numerical analysis, that the magnesium alloys have very limited formability at RT. However the formability can be improved when forming is carried out at higher temperatures. Finally, it can be concluded that the formability is improved as the punch radius and punch profile radius increase up to an optimum value and worsens with further increase.

ACKNOWLEDGEMENT

The authors are grateful to the European Commission for financial support under the contract Anon. AERONautical application of wrought MAGnesium (AEROMAG). EC/FP6 Growth/Aeronautics, 2005-2008.

REFERENCES

AERONautical application of wrought MAGnesium (AEROMAG), Research program, 2006.

Atkins, A.G., 1981, Possible explanation for unexpected departures in hydrostatic tension – fracture strain relations, *Journal of Materials Science*, 15, 81-83.

Brozzo, P., deLuka, B., Rendina, R., 1972, A new method for the prediction of Formability in sheet metals, *Proceedings of the seventh Biennial Conference on sheet Metal Forming and Formability 9th – 13th October Amsterdam,* International Deep drawing Research Group.

Ceretti, E., Fiorentino, A., Giardini, C., 2008, Process parameters influence on friction coefficient in sheet forming operations, *International Journal of Material Forming Supplement 1,* 1219- 1222.

Cockcroft, M.G., Latham, D.J., 1968, Ductility and the workability of metal, *Journal of the Institute of Metals,* 96, 33-39.

Chen, Fuh-Kuo, Huang, Tying-Bin, Chang, Chih-Kun, 2003, Deep drawing of square cups with magnesium alloy AZ31 sheets, *International Journal of Machine Tools and Manufacture*, 43, 1153-1559.

Furuya, H., Kogiso, N., Matunaga, S., Senda, K., 2000, Applications of magnesium-alloys for aerospace structure systems, *Journal of Materials Science Forum*, 350-351, 41-348.

Gotoh, M., Young-Soo Kim, Minoru Yamashita, 2003, A fundamental study of can forming by the stretch – drawing process, *Journal of Materials Processing and Technology*, 138, 545-550.

Hill, R., 1952, On discontinuous plastic states, with special reference to localized necking in thin sheets, *Journal of Mechanics and Physics of Solids,* 1, 19-30.

Marciniak, Z., Kuczynski, K., 1971, Limit strains in the processes of stretch forming sheet metal, *International Journal of Mechanical Sciences*, 13, 19-30.

Mordike, B.L., T. Ebert, 2001, Magnesium properties—application – potential, *Journal of Materials Science and Engineering*, 302(1), 37-45.

Nguyen, Ba, N., Bapanapalli, Satish, K., 2009, Forming analysis of AZ31 magnesium alloy sheets by means of multistep inverse approach, *Journal of Materials and Design*, 30, 992-999.

Norris Jr.,D. M., Reaugh, J. E., Moran, B., Quinones, D.F., 1978, A plastic strain, mean – stress criterion for ductile fracture, *Journal of Engineering Materials Technology – Transactions ASME*, 101, 279-286.

Oh, S.I., Chen, C.C., Kobayashi, S., 1979, Ductile fracture in axisymmetric extrusion and drawing, *Journal of Engineering for Industrial - Transactions ASME*, 100, 279-286.

Oyane, M., Sato, T., Okimoto, K., Shima, S., 1980, Criteria for ductile fracture and their applications, *Journal of Mechanical Working Technology*, 4, 65-81.

Ren, L.M., Zhang, S.H., Palumbo, G., Sorgente, D., Tricarico, L., 2009, Numerical Simulation on warm deep drawing of magnesium alloy AZ31 sheets, *Journal of Science and Engineering*, A, 499, 40-44.

Sih, G.C., 1985, Mechanics and Physics of Strain Energy Density, *Theoretical and Applied Fracture Mechanics*, 4 (4), 157-173.

Swift, H.W., 1952, Plastic instability under plane stresses, *Journal of the Mechanics of Solids,* 1, 1-18.

Takuda, H., Yoshii, T., Hatta, N., 1999, Finite Element analysis of the formability of a magnesium based alloy AZ31 sheet, *Journal of Materials Processing Technology*, 89-90, 135-140.

Yang, Lian-fa, Mori, Ken-ichiro, Tsuji, Hirakazu, 2008, Deformation behaviours of magnesium alloy AZ31 sheet in cold deep drawing, *Transactions of Nonferrous Metals Society of China*, 18 (1), 86-91.

Zhang, S.H., Zhang, K., Xu, Y.C., Wang, Z.T., 2007, Deep drawing of magnesium alloy sheets at warm temperatures, *Journal of Materials Processing Technology*, 185, 147-151.

OPTYMALIZACJA PARAMETRÓW GŁĘBOKIEGO TŁOCZENIA STOPÓW MAGNEZU

Streszczenie

Odkształcalność stopów magnezu jest ograniczona, szczególnie w temperaturze otoczenia, ze względu na ich heksagonalną upakowaną strukturę krystalograficzną (HPC – ang. hexagonal close packed). W temperaturze otoczenia, w sieci heksagonalnej działa tylko jedna płaszczyzną poślizgu - płaszczyzna podstawy. Z uwagi na znacznie większe ścinające naprężenia krytyczne inne systemy poślizgu nie działają,. Ponieważ odkształcenie plastyczne zachodzi na skutek działania tylko jednej płaszczyzny podstawy łatwo następuje utrata stateczności materiału i dochodzi do jego pęknięcia. Powoduje to znaczne ograniczenia w przeróbce plastycznej stopów magnezu na zimno. Z drugiej strony, wzrost odkształcalności wynikający z aktywowania dodatkowych systemów poślizgu jest obserwowany w temperaturach 1500^{o}C – 3000^{o}C. Dodatkowo zaobserwowano, że odkształcalność badanych stopów jest wrażliwa na prędkość odkształcenia. W niniejszym artykule, metody doświadczalne i symulacje metodą elementów skończonych zastosowano do opracowania metodyki określania zakresów odkształcalności stopów magnezu AZ31 i WE43. Zaproponowana metodyka opiera się na teorii gęstości energii odkształcenia. Na podstawie opracowanej metodyki wyznaczono optymalne parametry procesu głębokiego tłoczenia, takie jak promień stempla, temperatura, promil profilu i głębokość formowania.

Received: June 14, 2010
Received in a revised form: July 13, 2010
Accepted: July 20, 2010